Principles of Colloid and Surface Chemistry

Third Edition, Revised and Expanded

Paul C. Hiemenz
California State Polytechnic University
Pomona, California

Raj Rajagopalan
University of Florida
Gainesville, Florida

MARCEL DEKKER, INC. NEW YORK • BASEL

Library of Congress Cataloging-in-Publication Data

Hiemenz, Paul C.
Principles of colloid and surface chemistry. — 3rd ed., rev. and expanded / Paul C. Hiemenz, Raj Rajagopalan.
p. cm.
Includes bibliographical references and index.
ISBN 0-8247-9397-8 (hardcover : alk. paper)
1. Colloids. 2. Surface chemistry. I. Rajagopalan, Raj.
II. Title.
QD549.H53 1997
541.3'45—dc21

97-4015
CIP

The publisher offers discounts on this book when ordered in bulk quantities. For more information, write to Special Sales/Professional Marketing at the address below.

This book is printed on acid-free paper.

Marcel Dekker, Inc.
270 Madison Avenue, New York, New York 10016

Current printing (last digit):
10 9 8

PRINTED IN THE UNITED STATES OF AMERICA

$$H^+ + S_2O_3^{2-} \rightarrow HSO_3^- + S \qquad (B)$$

Slow growth on the original nuclei is how the narrow distribution of particle sizes is obtained, just as with the colloidal gold described in the preceding section. The formation of sulfur may be terminated at any time by adding I_2 to react with the remaining thiosulfate. These monodisperse sulfur sols have been studied extensively, notably by V. K. LaMer and coworkers. Since these particles are nonabsorbing in the visible spectrum, the range of particle sizes that may be conveniently dealt with is broader than for absorbing particles such as gold. Using the Mie theory, one can evaluate the scattering efficiency as a function of R_s for particles having a refractive index relative to the medium of 1.50, which describes the sulfur-water system.

These "monodisperse" sulfur sols are good examples of another light scattering phenomenon: the *higher order Tyndall spectrum*. We observed in Section 5.7a that the scattering cross section is an irregularly oscillating function of θ, at least above a certain threshold value of β. Here it should be recalled that the complete theory reduces to the Rayleigh approximation for very small particles and to the Debye approximation for somewhat larger particles, provided the refractive index values are in the proper range.

The full solution of the Mie theory provides quantitative information about the dependence of the efficiency factors on θ and λ. For uniform spheres over some range of refractive index and size, different colors of light will be scattered in different directions. The sulfur sols described here have the required properties to display this effect. Therefore, if a beam of white light is shown through a sample of the dispersion, various colors will be seen at different θ values. The resulting array of colors is known as the *higher order Tyndall spectrum* (HOTS). Red and green bands are most evident in the sulfur sols, and the number of times these bands repeat increases with the size of the sulfur particles. Therefore the number and angular positions of the colored bands provide a unique characterization of the particle size. In the monodisperse sulfur sols, for example, particles having a radius of 0.30 μm are expected to show red bands at about 60, 100, and 140°. Particles with a radius of 0.40 μm, on the other hand, show red bands at about 42, 66, 105, 132, and 160°. Particle size determinations based on observations of this sort agree well with those determined from electron microscopy. These sulfur sols are quite easy to prepare, and it is interesting to observe the development of higher orders in the Tyndall spectrum as the thiosulfate decomposition reaction progresses.

It was once thought that the appearance of HOTS was evidence in itself for the presence of a monodisperse system. The argument was that one particle size would scatter, say, red light, at a particular angle, whereas another particle size would have the same R_s value and therefore the same scattering behavior for light of a complementary color. The resultant would be the obliteration of any distinct color: The scattered light would appear white. Although there may indeed be fortuitous cancellations of this sort at certain angles, it is also possible for certain bands to reinforce each other. In general, then, it is best to say that polydisperse systems may show HOTS, but in this case the angular distribution of bands is a characteristic of the particle size distribution. The angular location and number of bands as determined theoretically for uniform particles may not be used to interpret the HOTS of a polydisperse system correctly.

5.8 DYNAMIC LIGHT SCATTERING

As mentioned in Section 5.1, so far we have focused on what are known as static scattering experiments; that is, the intensities used in the methods discussed until now are time-averaged intensities at any given angle θ. In general, however, the intensity accessible in a scattering experiment depends on time t as well, since the scattering centers are in constant random motion due to their kinetic energy. The variation of the intensity with time, therefore, contains information on the random motion of the particles and can be used to measure the diffusion coefficient of the particles. The measured diffusion coefficient can then be used to determine the size of the particle. The class of light scattering methods based on the time dependence of the scattered light intensity is known as *dynamic light scattering* (DLS), and a large body of work on various aspects of this technique has appeared in the literature in recent years (Brown

1993; Chu 1991; Schmitz 1990). For example, the dynamic version of the diffusing wave spectroscopy described in Vignette V is a form of DLS, although in diffusing wave spectroscopy the method of analysis is different in view of multiple scattering. Most of the advanced developments are beyond the scope of this book. However, DLS is currently a routine laboratory technique for measuring diffusion coefficients, particle size, and particle size distributions in colloidal dispersions, and our objective in this section is to present the most essential ideas behind the method and show how they are used for particle size and size distribution measurements.

5.8a Intensity Fluctuations and the Siegert Relation

In a typical scattering experiment, a detector measures the intensity of the scattered radiation over a period of time, say, t_n, in discrete steps of Δt (see Figure 5.16a). As shown in the figure, the intensity $i(s,t)$ fluctuates around an *average* value because of the random motions of the scatterers. Until now, we have denoted the average by simply $i(s)$ for convenience. To be precise, however, the average should be denoted by, say, $\bar{i}(s)$, and this is an average *over time*, t, defined as

$$\bar{i}(s) = \lim_{t_n \to \infty} \frac{1}{t_n} \int_0^{t_n} i(s,t)\, dt \approx \lim_{n \to \infty} \frac{1}{n} \sum_{j=1}^{n} i(s,j\Delta t) \tag{102}$$

where the limit $t_n \to \infty$ reminds us that the measurement should be made over a sufficiently large time for the average to be accurate.

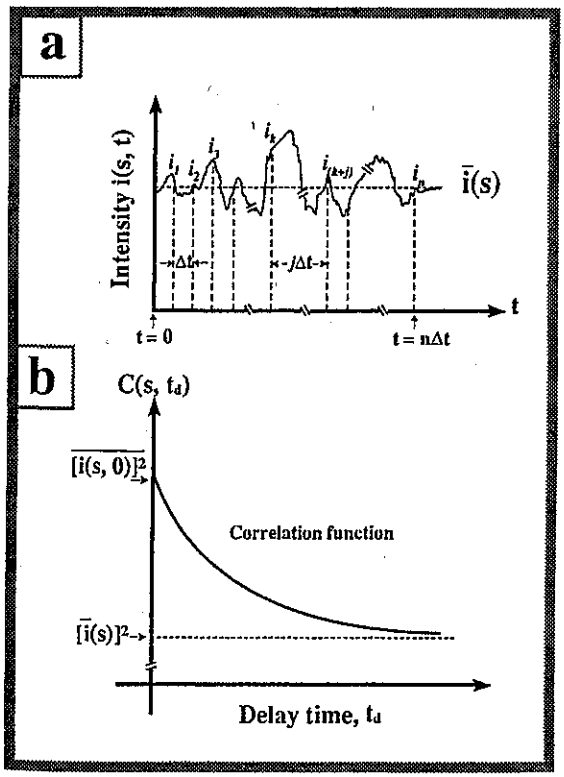

FIG. 5.16 Schematic illustration of intensity measurement and the corresponding autocorrelation function in dynamic light scattering: (a) variation of the intensity of the scattered light with time; (b) the variation of the autocorrelation function $C(s,t_d)$ with the delay time t_d.

Equation (102) also shows how the above time average is measured experimentally. Typically, the intensity is measured in a set of discrete time intervals, $t = \Delta t, 2\Delta t, 3\Delta t, \ldots$, etc., as illustrated in Figure 5.16a, and the arithmetic average shown in Equation (102) is an approximation of the average intensity over time $t_n = n\Delta t$.

In order to be able to use the *fluctuation* of the intensity around the average value, we need to find a way to represent the fluctuations in a convenient manner. In Section 5.3b in our discussion of Rayleigh scattering applied to solutions, we came across the concept of fluctuations of polarizabilities and concentration of scatterers and the role they play in light scattering experiments. In the present section, what we are interested in is the *time dependence* of such fluctuations. In general, it is not convenient to deal with detailed records of the fluctuations of a measured quantity as a function of time. Instead, one reduces the details of the fluctuations to what is known as the *autocorrelation function* $C(s,t_d)$, as defined below:

$$C(s,t_d) = \lim_{t_n \to \infty} \frac{1}{t_n} \int_0^{t_n} i(s,t)i(s,t + t_d)dt = \overline{i(s,0)i(s,t_d)}$$
$$\approx \lim_{n \to \infty} \frac{1}{n} \sum_{k=0}^{n} i(s,k\Delta t)i(s,(k + j)\Delta t) \tag{103}$$

where $t_d = j\Delta t$. The last part of the equation shows how the autocorrelation function is calculated experimentally when the intensity is measured in discrete time steps as illustrated in Figure 5.16a. The time t_d is known as the *delay time* since it represents the delay in time between the two signals $i(s,k\Delta t)$ and $i(s,(k + j)\Delta t)$ and is equal to $j\Delta t$ (see Figure 5.16a). The function $C(s,t_d)$ is obtained for a series of values of t_d by taking $j = 0, 1, 2, 3, \ldots$, etc. The autocorrelation function, as the name implies, is a measure of the correlation between the intensity $i(s,t_1)$ at any time t_1 and the intensity $i(s,t_1 + t_d)$ after a time *delay* of t_d. The correlation function obtained from Equation (103) is shown schematically in Figure 5.16b. Modern dynamic light scattering instruments consist of hardware "correlators" that have a number of channels or registers that keep track of $i(s,k\Delta t)$ for a large number of k's and automatically compute the products and the average in the summation term in Equation (103); see, for example, the schematic representation of a light scattering instrument shown in Figure 5.5.

The autocorrelation function has its highest value $\overline{[i(s,0)]^2}$ at $t_d = 0$. For $t_d \to \infty$, $i(s,t)$ and $i(s,t + t_d)$ become uncorrelated, and it can be shown that $C(s,t_d)$ is again independent of t_d and that it is given by $[\bar{i}(s)]^2$, where $\bar{i}(s)$ is the average value defined in Equation (102). For nonperiodic $i(s,t)$, $C(s,t_d)$ decreases monotonically from $\overline{[i(s,0)]^2}$ to $[\bar{i}(s)]^2$. Therefore, the ratio of the autocorrelation function to its asymptotic value $[\bar{i}(s)]^2$ can be written as

$$\frac{C(s,t_d)}{[\bar{i}(s)]^2} = g_2(s,t_d) = 1 + \xi|g_1(s,t_d)|^2 \tag{104}$$

an equation known as the *Siegert relation*, in which ξ is an instrumental constant approximately equal to unity.

The Siegert relation is valid except in the case of scattering volumes with a very small number of scatterers or when the motion of the scatterers is limited. We ignore the exceptions, which are rare in common uses of DLS, and consider only autocorrelations of the type shown in Equation (104). As mentioned above, modern DLS instruments use computer-controlled correlators to calculate the intensity autocorrelation function automatically and to obtain the results in terms of the function $g_1(s,t_d)$; therefore we only need to concern ourselves here with the interpretation of $g_1(s,t_d)$.

5.8b Dilute (Noninteracting) Dispersions

5.8b.1 Monosize Spherical Particles: Measuring Diffusion Coefficient and Particle Size

For dilute dispersions, i.e., those in which the interparticle spacing is so large that there are no particle-particle interactions, DLS simply measures the intensity fluctuations due to single-

particle motion. For monosize, spherical particles, one can show rigorously that $g_1(s,t_d)$ decays exponentially as follows:

$$g_1(s,t_d) = \exp(-s^2 D t_d) \tag{105}$$

Here, D, which is the quantity we seek from $g_1(s,t_d)$, is the diffusion coefficient of the particle (and s is the magnitude of the "scattering vector" defined in Equation (57)). We can now use the *Stokes-Einstein equation* (see Equation (2.32) and the accompanying comment) to obtain the particle radius R_H from D:

$$D = \frac{k_B T}{6\pi\eta R_H} \tag{106}$$

where η is the viscosity of the fluid, k_B is the Boltzmann constant, and T is the absolute temperature of the dispersion. The radius R_H measured in this manner is usually known as the *hydrodynamic radius* (hence the subscript H) since it relies on the Stokes coefficient, $6\pi\eta R_H$—a result from fluid (or, hydro) dynamics.

The measurement of the diffusion coefficient (and the hydrodynamic radius from D) is one of the most common uses of DLS, but the method can also be used as a nonintrusive technique for measuring the viscosity of a fluid. In this case, one uses "probe" particles with a known radius so that the unknown quantity in the Stokes-Einstein equation is η. More sophisticated uses of the DLS technique using essentially the above concept are discussed in specialized monographs (Brown 1993; Pecora 1985; Schmitz 1990). The diffusing wave spectroscopy mentioned in Vignette V also measures $g_1(t_d)$, but $g_1(t_d)$ in DWS is no longer a function of the angle θ since multiple scattering smears out the angle dependence of the intensity. As a result, the theoretical formalism needed for the analysis of the correlation function differs from what we have presented above and in Section 5.8b.2.

Example 5.5 illustrates one use of the DLS data.

* * *

EXAMPLE 5.5 *Determination of the Effective Diameter of an Enzyme Using Dynamic Light Scattering.* DLS analysis of a dilute solution of the enzyme phosphofructokinase in water at $T = 293$K leads to the following data for the correlation function $g_2(s,t_d)$:

$s^2 t_d \times 10^{-10}$ (m^{-2} s)	0.4	0.8	1.2	1.6	2.0	2.4
$g_2(s,t_d)$	1.75	1.6	1.47	1.375	1.298	1.236
$s^2 t_d \times 10^{-10}$ (m^{-2} s)	2.8	3.2	3.6	4.0	5.0	10.0
$g_2(s,t_d)$	1.188	1.148	1.119	1.093	1.052	1.003

Assume that the enzyme is roughly spherical and that the instrument constant ξ in the Siegert relation is unity and determine the hydrodynamic radius R_H of the enzyme. Given that the partial molar volume $\bar{V}$ of the enzyme is $0.74 \cdot 10^{-3}$ m^3/kg and the molecular weight M is $4.78 \cdot 10^2$ kg/mol, determine the "dry radius" R_s for the enzyme and obtain the ratio (R_H/R_s). Can the difference between R_H and R_s be attributed to the bound water on the enzyme? The viscosity η of water at 293K may be taken as 0.001 kg/m s.

Solution: The given DLS data can be used to obtain the intensity autocorrelation function $g_1(s,t_d)$ by rewriting the Siegert relation as follows:

$$\ln g_1(s,t_d) = \ln [g_2(s,t_d) - 1]^{1/2} - 1/2 \ln \xi$$

This leads to

$s^2 t_d \times 10^{-10}$ (m^{-2} s)	0.4	0.8	1.2	1.6	2.0	2.4
$\ln g_1(s,t_d)$	−0.118	−0.23	−0.35	−0.464	−0.58	−0.696
$s^2 t_d \times 10^{-10}$ (m^{-2} s)	2.8	3.2	3.6	4.0	5.0	10.0
$\ln g_1(s,t_d)$	−0.81	−0.93	−1.04	−1.16	−2.45	−2.9

Equation (105) shows that the plot of $\ln g_1(s,t_d)$ versus $s^2 t_d$ should give a straight line with a slope equal to the negative of the diffusion coefficient D of the enzyme. A plot based on the above data gives a straight line with a slope of $-2.88 \cdot 10^{-11}$ m^2/s and an intercept of −0.026. Therefore, the diffusion coefficient based on the data is

$$D = 2.88 \cdot 10^{-11}\ \text{m}^2/\text{s}$$

(The magnitude of the intercept implies that the instrumental constant ξ is roughly 0.95.)

From the Stokes-Einstein relation, Equation (106), we then get

$$\begin{aligned} R_H &= k_B T/(6\pi\eta D) \\ &= [1.38\cdot 10^{-23}\,(\text{J/K})\cdot 293\text{K}] \div [(6\pi)0.001\ (\text{kg/m s})\ 2.88\cdot 10^{-11}(\text{m}^2/\text{s})] \\ &= 74.4\cdot 10^{-9}\text{m} \end{aligned}$$

The "dry radius" R_s can be calculated from

$$\begin{aligned} R_s &= [(3/4\pi)\bar{V}M/N_A]^{1/3} \\ &= [3/4\pi)[0.74\cdot 10^{-3}(\text{m}^3/\text{g})4.78\cdot 10^2(\text{kg/mol})/6.02\cdot 10^{23}\text{mol}^{-1}]^{1/3} \\ &= 52\cdot 10^{-9}\,\text{m} \end{aligned}$$

The ratio (R_H/R_s) is therefore 1.43.

The source of this 43% difference between the "dry radius" and the hydrodynamic radius is unlikely to be the increase in diameter due to bound water. It is more likely that the shape asymmetry of the enzyme (i.e., the approximation that the enzyme is effectively spherical) is the source of the above difference. ■

* * *

5.8b.2 *Effect of Polydispersity: Measuring Size Distribution*

The DLS measurements can also be used in more complicated situations, for example, (a) when interparticle interactions are important, (b) for dispersions with particles of other shapes, (c) for monitoring coagulation, and (d) when the dispersion is polydisperse. In all these cases, a significant amount of modeling is often necessary to interpret the measured autocorrelation function, and we do not consider them here. Instead, we restrict our attention to a brief discussion of item (d) above, namely, polydisperse systems, since it is concerned with a problem of more routine interest.

In the case of a polydisperse system, the overall decay of the function $g_1(s,t_d)$ is determined collectively by the decay rate (i.e., s^2D) corresponding to *each particle* (notice that s^2D varies with the particle size as evident from the Stokes-Einstein relation). In principle, the decay function in this case can be written formally in a simple manner as a weighted average of all possible decays:

$$g_1(s,t_d) = \lim_{n\to\infty} \frac{1}{n} \sum_{j=1}^{n} w_j(s^2D_j)\exp(-s^2D_jt_d) \tag{107}$$

where $w_j(s^2D_j)$ is a weighting function determined by the amount of particles in size range j; that is, the decay of $g_1(s,t_d)$ for a polydisperse system is an appropriately averaged function of the monodisperse case given in Equation (105). A number of methods are available for determining the size distribution from the experimentally determined $g_1(s,t_d)$. One of the simplest is based on what is known as the cumulant expansion, i.e., a series expansion of ln $g_1(s,t_d)$, given by

$$\begin{aligned} \ln g_1(s,t_d) &= \sum_{n=1}^{\infty} k_n(s)\,\frac{(-t_d)^n}{n!} \qquad \text{in the limit } \tau_d \to 0 \\ &= -\bar{D}\,s^2\,t_d + \sigma^2 s^4\,\frac{t_d^2}{2!} + \text{higher order terms} \end{aligned} \tag{108}$$

where k_n is known as the *nth cumulant*. Equation (108) also shows that the first-order cumulant is related to the average diffusion coefficients of particles of all sizes (denoted here by $\bar{D}$) and the second-order cumulant to the standard deviation σ of the distribution of diffusion coefficients (see Chapter 1 and Appendix C for a discussion of standard deviation and some of the related statistical concepts).

Equation (108) is accurate only for small delay times and, in fact, the higher order terms obtained experimentally are not usually very reliable because of the "noise" in the data.

However, it does illustrate how one can determine an average particle size and a measure of the breadth of the distribution function from experimental data. A plot of $[\ln g_1(s,t_d)/(s^2t_d)]$ against (s^2t_d) will lead to a straight line for small t_d's, and $\bar{D}$ and s^2 can be obtained from the intercept and the slope of the straight line.

The logic of the above form of $g_1(s,t_d)$ and additional details are available in advanced books on DLS, and the above description is meant only to illustrate the basic ideas and one data-analysis approach. The cumulant analysis is often used as a first step before more advanced analytical procedures (each of which has its own advantages and disadvantages) are attempted. Most DLS instruments come with computer programs for the analysis of the size distribution, but we should bear in mind that each analysis technique has specific, and often restrictive, assumptions and none is "exact." As a consequence, the results of size distributions from DLS are best interpreted as semiquantitative indicators of polydispersity rather than a true representation of the distribution.

* * *

EXAMPLE 5.6 *Cumulant Analysis of Dynamic Light Scattering Data.* A polystyrene latex dispersion supplied by a manufacturer is claimed to have a "very narrow" size distribution with an average particle diameter of 62 nm. An analysis of the dispersion using DLS leads to the following data for $\ln g_1(s,t_d)$. The DLS experiments are conducted at 20°C using a dispersion in water at a particle volume fraction of 0.005. The wavelength of the laser used and the angle at which the experiments are conducted correspond to $6.5345 \cdot 10^6\ m^{-1}$ for the magnitude of the scattering vector s. The viscosity of water at 20°C may be taken as 0.001 kg/m s.

$t_d \times 10^3$ (s)	0.05	0.1	0.15	0.2	0.25
$\ln g_1(s,t_d)$	−0.015	−0.0305	−0.0457	−0.061	−0.076
$t_d \times 10^3$ (s)	0.3	0.35	0.4	0.45	0.5
$\ln g_1(s,t_d)$	−0.091	−0.107	−0.122	−0.137	−0.152

Check if the specifications supplied by the manufacturer are correct. State any assumptions you make in your evaluation of the data.

Solution: Assume that the interparticle forces are negligible. Further, since the volume fraction of the dispersion used in the DLS experiments is very low, we may assume that the dispersion is sufficiently dilute and that multiple scattering is negligible.

Equation (108) shows that the cumulant expansion for $\ln g_1(s,t_d)$ may be rearranged to give

$$y = \frac{\ln g_1(s,t_d)}{x} \approx -\bar{D} + \frac{\sigma^2}{2}x \qquad \text{with } x = s^2t_d$$

A plot of y versus x can now be used to obtain $\bar{D}$ from the intercept and σ^2 of the diffusion coefficient from the slope. Using the given data and the given value of s, we prepare a table of y versus x:

$x \times 10^{-10}$ (m^{-2} s)	0.2135	0.427	0.6405	0.854	1.0675
$y \times 10^{12}$ (m^2/s)	−7.03	−7.14	−7.135	−7.14	−7.15
$x \times 10^{-10}$ (m^{-2} s)	1.281	1.4945	1.708	1.9125	2.135
$y \times 10^{12}$ (m^2 s)	−7.10	−7.16	−7.14	−7.13	−7.12

It is clear from the table that the value of y is essentially constant over the entire range of given delay time. The slope, hence σ, is clearly negligible, and the intercept is approximately

$$\bar{D} = 7.14 \cdot 10^{-12}\ m^2/s$$

The use of the Stokes-Einstein relation with the above value of the average diffusion coefficient leads to a hydrodynamic radius of roughly 30 nm, which is consistent with the specification of the manufacturer. ■

* * *

5.8c Dispersions of Interacting Particles: Mutual and Self-Diffusion Coefficients

Even in the case of monodisperse systems, the observed decay rate of $g_1(s,t_d)$ (and hence the diffusion coefficient) in general depends on the angle at which the decay is measured if interparticle interference effects exist. In the case of *dilute* dispersions, in which interactions

of all sorts among the particles may be neglected, the interference is negligible, and the diffusion coefficient measured is independent of the angle and is given by the Stokes-Einstein equation (for spherical particles). This diffusion coefficient is often called the *self-diffusion coefficient* (or *probe diffusion coefficient*) since it represents the unhindered Brownian motion of a typical particle.

Although the analysis becomes complex for more concentrated dispersions (or even for dilute dispersions of charged particles, which can interact over very large distances), some general observations on two limiting cases are useful:

1. Measurements made at large enough values of Q ($= sR_s$) and for $t_d \to 0$: For $t_d \to 0$, the particles have very little time to wander far from their positions, i.e., the encounters with neighboring particles are negligible. Moreover, for large values of Q (e.g., large s) the interparticle interference is negligible since the range of interference in the observed intensity, represented by the magnitude of s^{-1}, is small. As a result, the measurements correspond again to the self-diffusion of the particles.

2. Measurements at low Q's: At low Q's, because of the large magnitudes of s^{-1}, the measured intensity and its autocorrelation function are dominated by the *cumulative* diffusion of the particles. The measured decay rate thus represents the *cumulative* or *mutual diffusion coefficient* D_m given by

$$D_m = \frac{1}{6\pi\eta R_s}\left(\frac{\partial \pi_{osm}}{\partial c_N}\right)_T \tag{109}$$

where π_{osm} is the osmotic pressure of the dispersion and c_N is the concentration of the particles in "number of particles/volume of dispersion." It is the cumulative diffusion coefficient that appears in the Fick's laws discussed in Chapter 2, and the diffusion experiments described in Chapter 2 measure this diffusion coefficient. Thus we have identified another method for measuring mutual diffusion coefficients for (at least spherical) solutes. For dilute dispersions, D_m in Equation (109) reduces to the self-diffusion coefficient. (Note that, for dilute systems, $\pi_{osm} = c_N k_B T$ and $(\partial \pi_{osm}/\partial c_N)_T = k_B T$.)

Moreover, the influence of the motions of the particles on each other (i.e., when the motion of a particle affects those of the others because of communication of stress through the suspending fluid) can also influence the measured diffusion coefficients. Such effects are called "hydrodynamic interactions" and must be accounted for in dispersions deviating from the dilute limit. Corrections need to be applied to the above expressions for D and D_m when particles interact hydrodynamically. These are beyond the scope of this book, but are discussed in Pecora (1985), Schmitz (1990), and Brown (1993).

We have made a note of the hydrodynamic interactions and other interactions to draw attention to an important fact. That is, the analysis of the DLS data is often quite complex, and a simple use of the single-exponential decay function and the Stokes-Einstein relation is not always sufficient, although many instruments available on the market use such an analysis and report an "effective size" for the particles in the dispersion.

REVIEW QUESTIONS

1. Describe briefly what is meant by light *scattering* and the mechanism by which molecules scatter light.
2. Explain what is meant by each of the following terms: (a) electric field, (b) intensity of light, (c) polarization of light.
3. What is *Coulomb's law* and what are the units of the quantities that appear in Coulomb's law?
4. Why is light scattering an important tool in colloid science? What is the range of dimensions of colloidal particles that can be probed by light scattering? Why?
5. What is the difference between *static* light scattering and *dynamic* light scattering?
6. How does light scattering differ from *x-ray* scattering and *neutron* scattering in terms of mechanisms as well as the range of interactions and structure that can be probed by each?
7. What is meant by *Rayleigh scattering*? What are the important assumptions and limitations of the Rayleigh theory?